Electronic Supplementary Material (ESI) for RSC Advances.

Dynamic electrochemical quantitation of dopamine release from a cell-on-paper system

Supporting Information

Raphaël Trouillon[a] and Martin A. M. Gijs[a]

Laboratory of Microsystems, Ecole Polytechnique Fédérale de Lausanne, CH-1015 Lausanne, Switzerland

In this file of Supporting Information, we provide further details on the chip and the experimental methods, as well as on the electrochemical characterisation of our system.

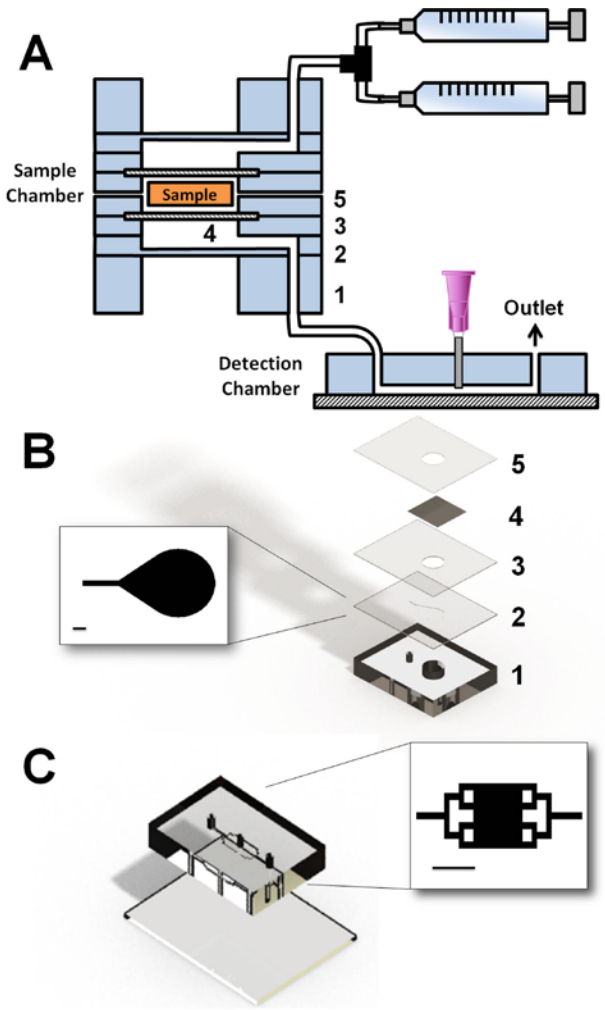

Figure S1: Description of the system. A- Scheme of the complete system (not to scale), with the two input syringes, the assembled sample chamber (the numbers correspond to the five layers that are described in the text) and the detection chamber, with the electrochemical sensor in place. B- Scheme of the fabrication of one half of the sample chamber. The numbers refer to the different layers shown in A. The picture on the left is the layout of the channels embedded in layer 2 (scale bar: 1 mm). C- Scheme of the fabrication of the detection chamber. The insert is the layout of the channels embedded in the PDMS layer (scale bar: 1 mm).

1- Experimental Methods

1.1 Chemicals

The chemicals and reagents, of analytical grade, were all obtained from Sigma-Aldrich (unless stated otherwise) and used as received. The HEPES physiological saline contains 150 mM NaCl, 5 mM KCl, 1.2 mM $MgCl_2$, 5 mM glucose, 10 mM HEPES, and 2 mM $CaCl_2$. The solution pH was adjusted to 7.4 with concentrated (3 M) NaOH. All solutions were made using 18 MΩ.cm water from a Millipore purification system.

1.2 Fabrication of the chips

The chips were initially designed in Clewin 4 and fabricated from PDMS using standard soft lithographic techniques.[1] Briefly, to make the master of the microfluidic system, a 100 µm thick SU-8 photoresist layer was spin-coated on a clean Si wafer, and patterned through a Cr mask. After developing and silane functionalization of the SU-8 master, a 10:1 poly(dimethylsiloxane) (PDMS) mixture was poured on the SU-8 structure and polymerized in an oven at 100 °C for 1 h. Also, a ~200 µm thick PDMS membrane was made by pouring the required quantity of uncured PDMS in a petri dish. To close the channels, the resulting patterned PDMS layer was bound to another PDMS surface or to a piece of clean microscope slide after surface-activation with air plasma (12 W for 70 s).

The sample chamber, where the cell-on-paper sample was inserted during the experiment, was made of two identical pieces described in Figure S1A and B, which were themselves made of five layers. First, a thick (~4 mm) piece of PDMS (layer 1) was used to provide mechanical strength to the system. This layer was pierced with a 6 mm hole using a biopsy puncher to allow gaseous and heat exchange. A second layer, featuring a 100 µm deep channel made of a 6 mm disk connected to a 100 µm wide microchannel (Figure S1B, left) was prepared. The approximate thickness of this layer was ~300 µm. Layer 2 was then bonded to layer 1, with the

channels facing up. As shown in Figure S1A, the lumen of the microchannel is separated from the atmosphere by a ~200 µm thick PDMS membrane, allowing gaseous and heat exchange. A fluidic connection was established by punching a Ø 1.5 mm porthole across layers 1 and 2. The microchannels are then closed by bonding layer 3, a ~200 µm thick PDMS membrane featuring a 6 mm hole. Layer 4 was a piece of porous polycarbonate membrane (3 µm pores, 11.3% overall porosity, Millipore, USA) closing the 6 mm hole pierced across layer 3. Uncured PDMS was carefully painted over the surface of layer 3 to allow for the bonding of the polycarbonate membrane. Finally, layer 5, which is similar to layer 3, was glued using PDMS over layers 3 and 4 to complete the device.

The detection chamber (Figure S1C) was simply made by bonding a ~4 mm thick piece of PDMS featuring the microfluidic system shown in the insert in Figure S1C. Before that, Ø 1.5 mm portholes were punched at each extremity of the chip, for the inlet and outlet, and a Ø 0.75 mm hole was punched in the centre of the 1 mm square present at the centre of the microfluidic design, to allow for the insertion of the sensor.

Fluid connections were completed by inserting tubings into the port holes. The fluid flows were actuated from a computer-controlled Nemesys system (Cetoni GmbH, Germany) featuring two low-pressure pump modules.

1.3 Electrode fabrication

The sensor was prepared by threading a Ø 51 µm Pt wire, Teflon coated, and a Ø 75 µm Ag wire, Teflon coated (both from Science Products GmbH, Germany) in the lumen of a 20 G blunt syringe needle (H. Sigrist & Partner AG, Switzerland).[2–4] The extremities of the wires were stripped of the Teflon with a flame and attached to connection wires using conductive silver paste. A third connection wire is also attached with silver paste to the metal of the needle. The lumen of the needle is filled with fluid epoxy (EPO-TEK 302-3M, Epoxy Technologies Inc., USA), to secure the wires in place, and the system is let to set overnight. The connections are then secured in place using heat-shrink tubings, and the tip of the needle is gently polished, finishing with 0.05 µm alumina slurry, to expose the three electrodes (Fig. 1B in the main article): the Pt working electrode (WE), the Ag|AgCl reference electrode (RE), and the stainless steel of the needle used as a counter electrode (CE).

1.4 Preparation of the electrode and electrochemical characterization

All the electrochemical tests were performed using an Ivium-stat potentiostat (IviumTechnologies, Netherlands). Before each set of experiments, the sensor was carefully polished with fine sandpaper and alumina slurry (0.05 µm particles). The sensor was then sonicated for 5 minutes in isopropyl alcohol. A layer of chloride was deposited on the Ag electrode by immersing the sensor in 3 M KCl. Several current steps (-20 µA for 1 s followed by 20 µA for 9 s) were applied for 1 min. The quality of the deposition was checked with a stereomicroscope (Fig. 1B in the main article). The sensor was finally inserted into the detection chamber, as shown in Fig. 1A, so that the electrodes are in the lumen of the channels. The WE was cleaned electrochemically in HEPES buffer (flow rate v= 1 µl s^{-1}) by running 20 cyclic voltammogram (CV) cycles from 0 V to 1.5 V (scan rate SR= 500 mV s^{-1}). A solution of 1 mM of DA in HEPES buffer was used, at a flow rate of 1 µl s^{-1}, to test the detection device, as described below.

1.5 Cell culture

PC12 cells were purchased from the European Collection of Cell Cultures. The cells were maintained in RPMI-1640 media supplemented with 10 % donor equine serum, 5 % foetal bovine serum, 2 mM L-glutamine and 0.4 % penicillin streptomycin solution in a 7 % CO_2, 100% humidity atmosphere at 37°C. The cells were grown on poly(L-lysine)-coated cell culture flasks and were sub-cultured every 7 days. The medium was replaced every 3 days throughout the lifetime of all cultures. Cells from generations 10 to 15 were used in this study.

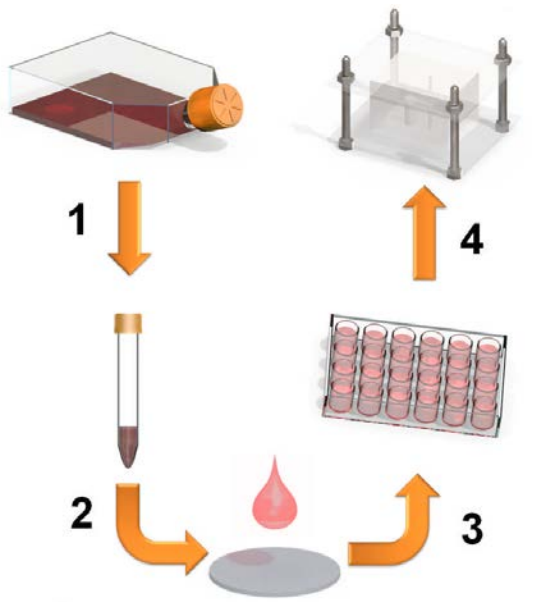

Figure S2: Preparation the cell-seeded paper patches and data processing. Cultured cells are harvested and resuspended in a mixture of ECM gel and medium at a density of 1 x 10^8 cells ml^{-1} (step 1), 5 µl of this preparation is deposited on a clean paper patch and allowed to gel (step 2). The cell-seeded paper patches are cultured for 2-4 hours in medium, in absence or presence of drugs (step 3) before being inserted in the sample chamber for the detection experiment (step 4).

1.6 Preparation of the cell-seeded paper patches

The PC12 cells were seeded on paper patches using a modified version of a method described by others.[5,6] The protocol for the preparation of the paper samples is summarized on Fig. S2. The paper patches were cut in a sheet of paper (filter paper 114, Whatman, UK) with a ~5 mm punch. The patches were cleaned successively by 10 min sonication in water and 70% ethanol, and then dried and sterilized in an oven at 120

˚C for at least 6 hours. Confluent PC12 cells were harvested mechanically from a flask and counted. After centrifugation, the cells were re-suspended in media to achieve a cell concentration of 2 x 10^8 cells ml^{-1}. The cell solution was mixed, in a 1:1 ratio, with cold (4˚C) extracellular matrix (ECM) gel from Engelbreth-Holm-Swarm murine sarcoma. A 5 µl drop of the cell/ ECM gel mixture was then deposited on each of the paper patches, which have been previously placed in individual wells of a 24-well plate. After 2-5 min in the incubator to allow gelation, media was added to each well containing a seeded paper disk.

For the L-DOPA treatment, the plate was then incubated for 2-4 hours in presence, if applicable, of 100 µM L-DOPA. For the dynasore experiments, a 100 mM stock solution was prepared by dissolving dynasore hydrate in DMSO (the MW of anhydrous dynasore was used for this dilution). The cells were then exposed to HEPES buffer containing the appropriate quantity of dynasore for 5 minutes.

1.7 Fluorescence imaging of the cell-seeded paper patches

The paper patches containing cells were fixed for 10 minutes in acetone at -20 ˚C. Some of the patches had been previously placed in the cell chamber and exposed to a flow of HEPES buffer (1 µl s^{-1}) for 10 mins. The fixed patches were rinsed and stored in PBS at 4 ˚C. Just before the imaging, the paper patches were deposited on a clean microscope slide and mounted with Fluoroshield mounting medium containing 4',6-diamidino-2-phenylindole (DAPI). The samples were imaged with an Image 2M microscope (Carl Zeiss) using the 5x and 10x objectives. A mosaic algorithm was used to reconstruct the overall image of the patch from smaller tiles.

1.8 DA release experiment

The calibration of the complete system was performed by injecting in the assembled system plugs of 1 mM DA at 1 µl s^{-1}, repeated every 2-4 measurements to track the changes in sensitivity. In that configuration, the sample chamber was empty or filled with a paper patch without cells.

To perform cell measurements, the detection chamber is first filled with buffer, and the WE is poised at 0.7 V *vs.* Ag|AgCl until the recorded signal is stable. In the case of the experiments involving dynasore, the inhibitor was also added to the HEPES buffer at the relevant concentration to avoid reversal of the inhibiting effect. Then, a paper patch loaded with cells is placed in the sample chamber. The two halves of the chip are assembled and held together using a custom holder (step 4 in Fig. 2A). The sample chamber is connected to the two input 1-ml plastic syringes, placed in the syringe pump, using a T-junction and ~10 cm of tubing. HEPES is injected into the system at 1 µl s^{-1} to fill the chamber and remove air bubbles. The sample chamber is then connected, using ~10 cm of tubing, to the detection chamber. HEPES is continuously injected at 1 µl s^{-1} for 1 min to flush away air bubbles, and the system is carefully checked for leaks. Once the system is ready, a stream of 100 µM ACh (in HEPES buffer) is injected and the recording of the electrochemical signal is initiated simultaneously. After 400 s, the ACh flow is stopped, and HEPES buffer is injected at 1 µl s^{-1}. The experiments were carried out at room temperature, and the sampling frequency was 1 Hz.

1.9 Data processing

As detailed below, the dead-volume time T_{DV}, *i.e.* the delay between the injection of a plug of DA and the time when it is detected by the potentiostat, is subtracted from the time axis, so that 0 s corresponds to the time when the stimulating buffer enters the detection chamber.

The traces were filtered with a median filter over 11 points, where the outliers differing by more than one median from the median value are replaced with the median. This first filter is used to remove peak-shape artefacts, typically due to convection noise. The trace is then further smoothed with a binomial filter, over 11 points. The baseline is fitted with a decaying exponential and subtracted from the signal and converted to concentration using the calibration data. The section of the recorded data normally corresponding to the detection of DA is not taken into account in the background fitting.

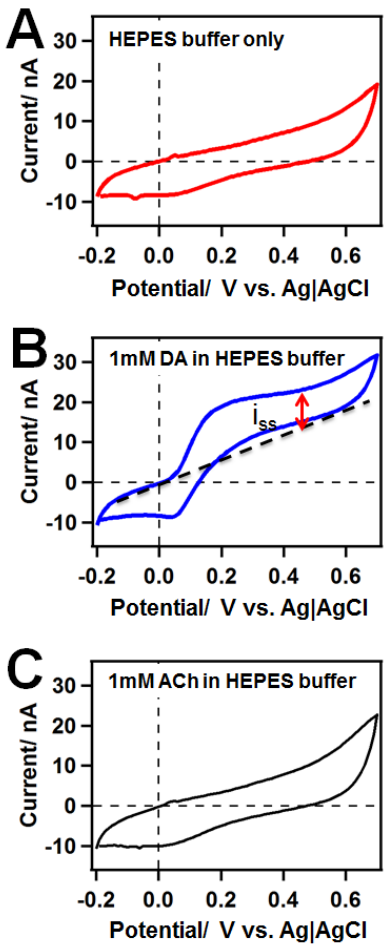

Figure S3: Typical CV (*SR*= 100 mV s^{-1}) in A- HEPES buffer, B- 1 mM DA in HEPES buffer and C- 1 mM ACh in HEPES buffer. In this set of experiments only, the solutions were degassed with nitrogen.

Several parameters were extracted from each of the individual traces, as shown on Fig. 3D. The maximum concentration, usually observed as a peak, is C_{max}. The delay time t_{delay} is

the time at which the signal exceeds the baseline by 3 times the SD of the background. The rise time t_{rise} is the time separating the point where the signal is 25% of C_{max} from the time where the signal is 75% of C_{max}, on the ascending part of the curve. Finally, the area under the curve, obtained by integrating the signal, is multiplied by v and by Avogadro's number to obtain the number of molecules released by the cells since the onset of the stimulation until the end of the experiment at 500 s, defined as N_r. Where applicable, the data are reported as average ± standard deviation (SD), and the number of individual measurements is described using the notation n. Comparisons between different datasets was performed with a two-tailed Student's t-test, assuming equal variances, or a 1-way ANOVA, depending on the type of dataset.

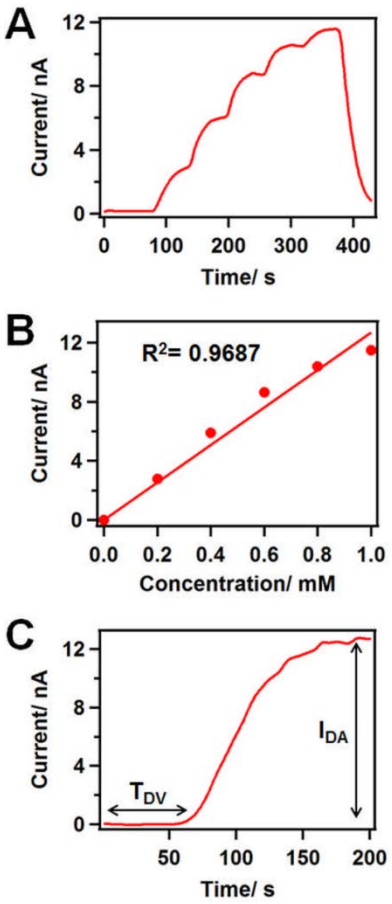

Figure S4: Amperometric response of the assembled system to DA injection. A- Calibration trace performed by injecting 60-s steps of DA solution by increments of 0.2 mM (v= 1 µl s-1, electrode potential: 0.7 V vs. Ag|Agcl). B- Calibration curve corresponding to the trace shown in panel A. A linear fit was added to emphasize the linear behaviour. C- Injection at 1 µl s^{-1} of a 1-mM step of DA, showing the two parameters extracted for the system characterization, T_{DV} and I_{DA}.

2- Electrochemical characterisation

The electrochemical performances of the sensor were investigated with CV in free HEPES buffer volumes, outside of the microfluidic system. In this set of experiments, the solutions were degassed with nitrogen to avoid interferences due to the reduction of dissolved oxygen, which was not possible in the microfluidic configuration.

Typical CVs obtained from the needle sensor are reported in Figure S3. Figure S3A shows a typical CV (SR= 100 mV s^{-1}) in pure HEPES buffer. No obvious Faradaic signal can be observed, and this trace corresponds to the control. In presence of 1 mM DA (Figure S3B), a clear signal was observed for potentials above ~0.1 V vs. Ag|AgCl, corresponding to the two-electron oxidation of DA to dopamine-*o*-quinone. A small peak can still be observed, but the shape of the voltammogram is largely similar to a sigmoid. This shape is in agreement with standard electrochemistry and is characteristic of the spherical diffusion layer expected at a microelectrode. The steady-state current i_{ss} associated to DA oxidation, which is defined in Figure S3B and can be seen after the peak, was here 12.4 nA. The theoretical expression of i_{ss} is[7]

$$i_{ss} = 4NFDC_0r_0 \qquad (1)$$

where N is the number of electrons exchanged, F is the Faraday's constant, D is the diffusion coefficient of the analyte (here, D was taken as 6.0 10^{-10} m^2s^{-1}),[8] C_0 is the concentration of the analyte and r_0 is the radius of the electrode. Overall, the theoretical value of i_{ss} is 11.8 nA, in good agreement with the experimental data. The current i_{ss} was chosen here over the peak current mostly because the observed peak is small. Moreover, this value is expected to be more relevant to our analysis as amperometry, which functions in a steady-state and diffusion-limited regime, is used. Furthermore, as shown in Figure S3C, no clear signal can be observed when the CV is ran in a solution of 1 mM ACh, and the trace is largely identical to the one obtained for control. This shows that the introduction of ACh into the system does not elicit any strong response and that ACh can be used as a stimulant for the cells without dramatically affecting the electrochemical detection.

The response of the sensor to DA, functioning in the amperometric modality, was also checked in the complete assembled system. To achieve quantitative measurements of DA release, it is critical to perform calibration of the system in operating conditions, especially as the signal is dependent on hydrodynamic parameters.[7,9,10] As shown in Figure S4A, steps of increasing DA concentrations (increments of 0.2 mM) were injected in the device at a constant flow rate (1 µl s^{-1}). This was performed by modulating the relative flow rates of two input streams of solutions (pure HEPES buffer and 1 mM DA in HEPES buffer) so that the sum of the flow rates is fixed at 1 µl s^{-1}. The electrode potential was held at 0.7 V *vs.* Ag|AgCl which is sufficiently high (according to the CV shown in Figure S3B) to guarantee a diffusion-limited regime, even in case of minor drifts of the RE. The increases in current for each level, in comparison to baseline, were measured and plotted as a function of concentration to obtain the calibration curve shown in Figure S4B. This plot largely shows a linear behaviour, as indicated by the linear fit (R^2= 0.9687). As a consequence, the sensitivity of the system (*i.e.* the slope of the calibration curve) can be easily estimated by injecting a plug of 1 mM DA and measuring the magnitude of the current increase in comparison to the baseline, I_{DA} in Figure S4C. This is similar to a two-point calibration.

Furthermore, the dead-volume time, T_{DV}, separating the beginning of DA injection into the system from the onset of

the rise in current corresponding to DA oxidation was measured. This corresponds to the time needed for a plug injected into the system to travel across the device and reach the sensor. Please note that T_{DV} accounts for a technical parameter, *i.e.* the dead volume in the system, and is different from t_{delay}, which is biologically relevant and describes the lag time between the onset of the cell exposure to ACh and the beginning of a detectable DA release. Neither I_{DA} nor T_{DV} were found to be dependent on the presence of patch of paper in the sample chamber (data not shown). The sensitivity was found to depend largely on the placement of the sensor in the channel (*i.e.* if it is closer to the walls or closer to the centre of the channel). Overall, for the average of 19 measurements, the sensitivity was 25.0 ± 12.9 nA mM^{-1} and the limit of detection (LoD), defined as the concentration corresponding to a signal level equal to three time the standard deviation of the baseline, was 4.6 ± 8.9 nM. Lower LoDs have been reported for similar systems, but the LoD obtained with our device is nevertheless two orders of magnitude below the DA experimental signal (in the 100 nM range, see the main manuscript) and sufficient for our analysis. As a consequence, we have not tried to lower the LoD any further, even though several strategies could be implemented (electromagnetic screening, more stringent filtering, *etc.*). The high level of variability was attributed to the differences in electrode positioning during the assembling of the system. A possible strategy for improving the positioning of the electrode, and therefore the reproducibility of the system, would be to use 3D printing to design the detection chamber and avoid the use of elastomer.[11] However, this calibration was repeated before each set of 2-4 experiments and the detection chamber was not manipulated once it has been calibrated. This strategy ensures the sensitivity does not drift over the course of the experiment.

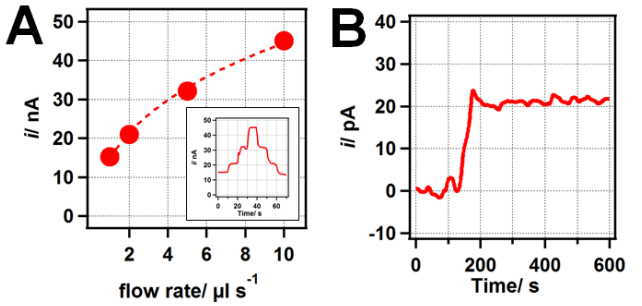

Figure S5: A- Effect of the flow rate *v* on the measured current (1 mM DA in HEPES buffer, electrode potential 0.7 V, *v*= 1, 2, 5 and 10 µl s^{-1}). The fitted curve (dashed line) is the cube root of *v*. The insert is the experimental trace. B- Injection of 1 µM DA in HEPES at 1 µl s^{-1}, the electrode potential was 0.7 V. The black bar shows the section of the curve corresponding to the DA injection. Here, the background current was subtracted. The signal is stable over ~500 s, thus showing the absence of dramatic electrode fouling.

The effect of the flow rate *v* on the measured signal is shown in Figure S5A. Here, the electrode potential was fixed at 0.7 V, and the system was filled with a 1 mM DA solution (in HEPES buffer). The current was measured as *v* was varied stepwise to 1, 2, 5 and 10 µl s^{-1}, before being decreased in the same manner back to 1 µl s^{-1}. The amperometric trace is largely symmetric, thus showing the good reproducibility of the system. The currents associated to each *v* value, on the ascending part of the graph, were plotted as a function of *v*. The current was here found to be well fit with the cube root of *v*. This is in good agreement with the electrochemical theory, where the flux of analyte (or the current) is proportional to the concentration gradient, which is itself proportional to the invert of the thickness of the diffusion layer.[12,13] Under hydrodynamic conditions, the thickness of the diffusion layer is proportional to $v^{-1/3}$, and as a consequence, the variations of the current with *v* should be described by $v^{1/3}$, in good agreement with our experimental data.

Moreover, electrode fouling potentially can be a critical problem for electrochemical sensing, especially in presence of DA. Indeed, oxidised DA is known to polymerise and form an insulating film on the electrode surface. Here, in Figure S5B, a stream of HEPES was injected, followed by 1 µM DA in HEPES, always at 1 µl s^{-1}. This concentration was chosen, because it is of the same magnitude as the maximum concentration detected for the PC12-seeded paper patches. This trace was background-subtracted. The electrode was held at 0.7 V, and all the other parameters were similar to the ones used to the electrochemical detection. This experiment reveals that the current is stable for ~500 s, which is the duration of the measurements. Should a significant electrode fouling happen, a decrease in current would be observed. This is not the case here, thus showing that the low concentrations encountered during the experiment limit the impact of electrode fouling.

References

(1) Xia, Y.; Whitesides, G. M. *Annu. Rev. Mater. Sci.* **1998**, *28* (1), 153–184.

(2) Patel, B. A.; Rogers, M.; Wieder, T.; O'Hare, D.; Boutelle, M. G. *Biosens. Bioelectron.* **2011**, *26* (6), 2890–2896.

(3) Rogers, M. L.; Feuerstein, D.; Leong, C. L.; Takagaki, M.; Niu, X.; Graf, R.; Boutelle, M. G. *ACS Chem. Neurosci.* **2013**, *4* (5), 799–807.

(4) Bitziou, E.; O'Hare, D.; Patel, B. A. *Anal. Chem.* **2008**, *80* (22), 8733–8740.

(5) Derda, R.; Laromaine, A.; Mammoto, A.; Tang, S. K. Y.; Mammoto, T.; Ingber, D. E.; Whitesides, G. M. *Proc. Natl. Acad. Sci.* **2009**, *106* (44), 18457–18462.

(6) Derda, R.; Tang, S. K. Y.; Laromaine, A.; Mosadegh, B.; Hong, E.; Mwangi, M.; Mammoto, A.; Ingber, D. E.; Whitesides, G. M. *PLoS ONE* **2011**, *6* (5), e18940.

(7) Bard, A. J.; Faulkner, R. L. *Electrochemical Methods: Fundamentals and Applications*, 2nd ed.; John Wiley and Sons: Hoboken, NJ, USA, 2001.

(8) Gerhardt, G.; Adams, R. N. *Anal. Chem.* **1982**, *54* (14), 2618–2620.

(9) Trouillon, R.; Gijs, M. A. M. *Lab. Chip* **2014**, *14*, 2929–2940.

(10) Trouillon, R.; Gijs, M. A. M. *Electrochimica Acta* **2015**, *166*, 223–231.

(11) Gowers, S. A. N.; Curto, V. F.; Seneci, C. A.; Wang, C.; Anastasova, S.; Vadgama, P.; Yang, G.-Z.; Boutelle, M. G. *Anal. Chem.* **2015**.

(12) Levich, V. G. *Physicochemical hydrodynamics*; Prentice-Hall: Englewood Cliffs, N.J, 1962.

(13) Probstein, R. F. *Physicochemical Hydrodynamics: An Introduction*, 2nd Ed.; Wiley-Interscience: Hoboken, N.J., 2003.